Journal of Power Sources 189 (2009) 1023–1031

Contents lists available at ScienceDirect

Journal of Power Sources

journal homepage: www.elsevier.com/locate/jpowsour

Gas–liquid two-phase flow distributions in parallel channels for fuel cells

Lifeng Zhang[a], Wei Du[a], Hsiaotao T. Bi[a,*], David P. Wilkinson[a], Jürgen Stumper[b], Haijiang Wang[c]

[a] Department of Chemical and Biological Engineering, The University of British Columbia, 2360 East Mall, Vancouver, Canada V6T 1Z3
[b] Automotive Fuel Cell Corporation, 9000 Glenlyon Parkway, Burnaby, BC, Canada V5J 5J8
[c] NRC Institute of Fuel Cell Innovation, Vancouver, Canada

ARTICLE INFO

Article history:
Received 12 November 2008
Received in revised form 5 January 2009
Accepted 7 January 2009
Available online 19 January 2009

Keywords:
Flow distribution
Flow hysteresis
Parallel minichannels
Gas–liquid two-phase flow
Flow stability
Fuel cells

ABSTRACT

In the present study, gas–liquid two-phase flow in a parallel square minichannel system oriented horizontally and at an incline is studied under operating conditions relevant to fuel cell operations. Flow mal-distribution in parallel channels occurs at low gas and liquid flow rates. In general, high superficial gas velocities are required to ensure even flow distribution, and the minimum gas flow rates required to achieve even distribution depend on the liquid flow rates, channel orientation and experimental procedures. As the inclination angle is increased, a higher gas flow rate is required to ensure even gas–liquid flow distribution while flow channels inclined downward seems to help in improving the even flow distribution. The presence of flow hysteresis phenomena indicate that multiple flow distributions exist at the same given flow conditions when the gas flow rates are varied in ascending and descending manners. Flow mal-distribution and flow hysteresis are directly linked with flow stability. More specifically, the actual gas and liquid distribution in parallel channels is determined by the stability of mathematical solutions of mass and momentum balance equations and also the flow history. For the first time, the present work investigates flow distributions in fuel cell flow fields by accounting for two-phase flow conditions. In addition, a novel approach is introduced to ensure flow distributions and their stability through contour construction of isobars where unstable flow region can be identified, which can be used in the design of parallel channel flow fields, especially for fuel cells.

1. Introduction

Gas–liquid flow in parallel channels has received much attention due to their importance in practical engineering applications such as heat exchangers, condensers and fuel cells. Particularly, in fuel cell flow fields, there will be generally a common manifold at the inlet and or at the outlet and even distribution of gas and liquid into parallel channels is always desired. However, non-uniform flow distribution is still an issue encountered in fuel cell applications, leading to severe pressure drop and performance fluctuations in polymer electrolyte membrane fuel cells (PEMFCs). One channel might be flooded with water while other channels are dried out with an excess amount of gas reactant. Several attempts have been made to model and predict flow distribution in parallel channels related to fuel cell applications [1–3]. However, the hydrodynamic model is developed solely based on a single phase gas flow and is not suitable for two-phase flow systems where various possible gas and liquid flow combinations can give the same pressure drop. Therefore, in PEMFC applications, particularly, at higher current densities or low gas stoichiometry, liquid water is most likely present and a two-phase flow system is encountered in the flow field and head distributor. However, only very few studies are reported concerning the effects of flow mal-distribution on PEMFC power performance [4,5]. A thorough understanding of mechanism underlying flow mal-distribution is still lacking in the open literature.

In the literature, there are a few studies on gas–liquid flow distribution in parallel channels/pipes for other engineering applications [6–10]. However, most of studies have focused on high gas and liquid flow rates which are not relevant to fuel cell applications either due to too high a liquid flow rate (too high a current density) or too large a gas stoichiometry. As noted earlier, different from a single-phase flow, various combinations of gas and liquid flow rates can give a similar pressure drop. Theoretically, even distribution is always a solution to providing the equal pressure drop in parallel channels. However, depending on the operating regime, the flow distribution might not be stable and a small disturbance in flow rates can result in a persistent deviation from the even distribution. Therefore, even flow distribution is not always observed in experiments and instead flow mal-distribution occurs.

Ozawa et al. [11] studied flow instabilities in Y-branched parallel channels of 3.1 m in length and 3.1 cm in diameter. It was reported that even distribution took place in the range where pressure drop versus flow rate increased monotonically. When the superficial gas velocity exceeded 1.5 m s^{-1}, even distribution occurred.

* Corresponding author. Tel.: +1 604 822 4408; fax: +1 604 822 6003.
E-mail address: xbi@chml.ubc.ca (H.T. Bi).

0378-7753/$ – see front matter © 2009 Elsevier B.V. All rights reserved.
doi:10.1016/j.jpowsour.2009.01.010

It was speculated that the flow mal-distribution is closely associated with negative pressure drop versus flow rate. Minzer et al. [8,9] reported that several possible stable solutions exist in practice and the stable solution depends on the inlet flow rate history, namely, increasing or decreasing the flow rate, leading to a flow hysteresis phenomenon. Previous studies also showed that flow mal-distribution in parallel channels was largely influenced by the gravitational effect. With an increase in inclined angles, even flow distribution occurred at higher gas flow rates.

Taitel et al. [7] investigated experimentally the distribution of gas–liquid two-phase flow in four parallel pipes with a common manifold. They reported that multiple gas and liquid flow combinations satisfied the equal pressure drop requirement. However, no flow hysteresis was observed in their study presumably due to the choice of their experimental conditions, especially the liquid flow rate, which was generally higher than 0.01 m s^{-1}. According to our previous work [12], hysteresis phenomena will more likely occur at low liquid and gas flow rates. We thus postulated that the actual solution, usually the experimentally observed one, might be defined by the minimal pressure drop of the system. The conclusion holds for the flow range where there exists a monotonic positive slope of the pressure drop versus gas velocities curve, but may not hold over the range when there exists a negative slope [8,9,11,12]. Pustylnik et al. [10] employed a linear stability analysis to predict the stability of a number of pipes of a stagnant liquid column. A simplified hydrodynamic model was developed based on momentum conservation, and a perturbation analysis was performed to examine the stability of the solutions. Experimental work was based on four horizontal pipes which were 2.6 cm in diameter and 6 m in length. The model prediction qualitatively agreed with their experimental work. However, a constant gas to liquid flow ratio in each pipe was assumed and a constant frictional factor was used in their model prediction. It should be noted that the above approach for turbulent flow in pipes is not suitable for the typical laminar flow regime encountered in fuel cells where the frictional factor varies with flow conditions.

In our previous work [12], gas–liquid two-phase flow patterns in parallel channels were reported under flow conditions relevant to fuel cell operations. It was found that flow hysteresis and flow mal-distribution in parallel channels occurred at relatively low gas and liquid flow rates. However, more detailed data on effects of operating variables on flow mal-distribution in parallel channels was not included. In fact, the present work is an extension of our previous work [12] and aimed at developing an improved understanding of flow mal-distribution in fuel cell flow channels.

In general, two-phase flow mal-distribution requires further studies, and in particular for minichannels of dimensions relevant to fuel cell applications. A better understanding of the mechanism of flow mal-distribution and flow hysteresis phenomena in two-phase flow systems is still lacking. Therefore, the objectives of the present study are to systematically investigate flow instability-induced flow mal-distribution in two parallel minichannels as a function of flow conditions and angle of inclination and to present a novel theoretical approach to predict stability of two-phase flow distributions through pressured drop calculations based on momentum balance.

2. Experimental

The experimental setup is schematically shown in Fig. 1. The experiments were conducted in Y-branched parallel square channels of 1.59 mm × 1.59 mm in cross-section. The channels were fabricated in a clear acrylic plate using a conventional milling machine. The length of the straight section of the parallel channels was 300 mm, and the branch section was 50 mm in length with a branch-out angle of 30°. An introduction channel of 3.2 mm in width, 1.59 mm in depth and 100 mm long connected the Y-branch to the inlet.

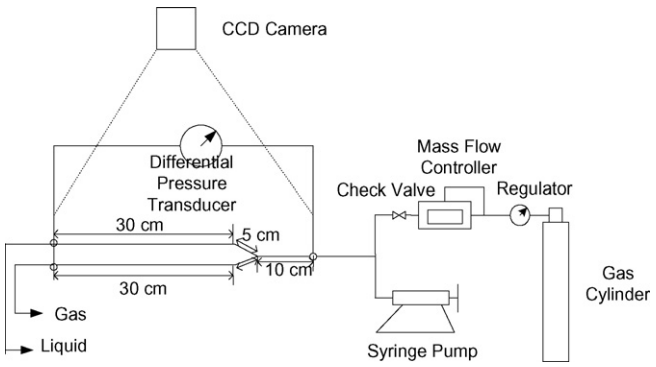

Fig. 1. Schematic of the experimental setup.

Air was supplied through a pressurized gas cylinder and the gas flow rate was measured through a mass flow meter (AALBORG, GFM17), with a maximum flow rate of 5 SLPM. A check valve was installed in order to protect water back flow into the mass flow meter. Water was injected into the channels by a syringe pump (Cole-Parmer 74900-00) with a maximum flow capacity of 350 ml h^{-1}. The pressure drop across the test section was measured by a micro switch differential pressure drop transducer with a maximum pressure difference range of 2000 Pa. Visualization of the two-phase flow was conducted with a Canon CCD camera at a standard frame speed of 30 frames s^{-1}.

During the course of experiments, the gas and liquid flow rates were controlled within typical operating conditions of active PEM fuel cells, with the superficial gas velocity ranging from 0 to 10 m s^{-1} and the superficial liquid velocity from 0 to 0.03 m s^{-1}, resulting in Reynolds numbers of 1–150 for the liquid phase and 10–1000 for the gas phase, respectively.

Under current operating conditions, the capillary number defined by

$$C_a = \frac{\mu_L u_L}{\sigma} \quad (1)$$

where μ_L is the liquid viscosity, Pa s, u_L is the superficial liquid velocity, m s^{-1} and σ is the liquid surface tension, ranges from 10^{-5} to 10^{-3}. This indicates a dominant effect of surface tension over the viscous force. These test conditions correspond to fuel cell operating conditions with equivalent current densities of 0–10 A cm^{-2} and a maximum stoichiometric ratio of 50. For a constant liquid velocity, the gas velocity was changed using two different experimental approaches. In the first experiment, the initial flow was pure water, and the gas velocity was increased from an initial gas flow rate of zero to simulate initial flooding conditions. However, in the second experiment, the gas flow rate was decreased from an initial maximum gas flow rate at a given liquid flow rate, corresponding to a dry condition.

In the current experimental conditions, the flow mainly falls into slug flow, slug-annular flow, and stratified flow regimes. Liquid holdup was also measured, especially, in the slug and slug-annular flow regimes, by capturing the number of liquid slugs within a set period of time, typically, in 5 min and then evaluated by the following equation:

$$\varepsilon_L = \frac{f_{slug} L_{slug}}{u_{slug}} \quad (2)$$

where f_{slug} is the slug frequency (Hz), L_{slug} is the length of liquid slugs (m) and u_{slug} is the slug velocity (m s^{-1}).

In order to characterize flow mal-distribution, liquid flow distribution was measured by collection and weighting of

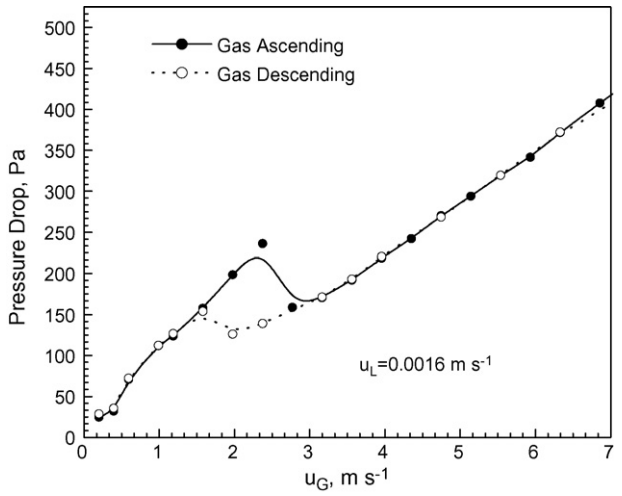

Fig. 2. Pressure drop versus gas velocities at $u_L = 0.0016\,m\,s^{-1}$ ($\beta = 0^\circ$).

water at the channel outlet over a given period of time and weighted.

3. Experimental results and discussion

3.1. Pressure drop

3.1.1. Effects of liquid flow rates on pressure drop

A typical pressure drop versus gas flow rate curve is shown in Fig. 2. The pressure drop is seen in Fig. 2 to initially increase with an increase in gas flow rates. However, a sudden drop in the pressure drop occurs at around $u_G = 2.8\,m\,s^{-1}$ in the gas ascending process, corresponding to a change in flow patterns in the two parallel channels from a non-uniform distribution to uniform flow in the two channels. With further increase in the gas flow rates, the pressure drop increases again, with an even distribution. When the experiment starts from a dry condition in the parallel channels, that is, at a high gas flow rate to ensure stratified flow conditions and following gas velocity descending process, the pressure drop trajectory does not completely follow the same path as in the gas ascending process, resulting in a hysteresis.

Similar phenomena were observed at a higher liquid velocity of $u_L = 0.0033\,m\,s^{-1}$, as shown in Fig. 3, although an even distribution is achieved at lower gas flow rates, resulting in a narrower

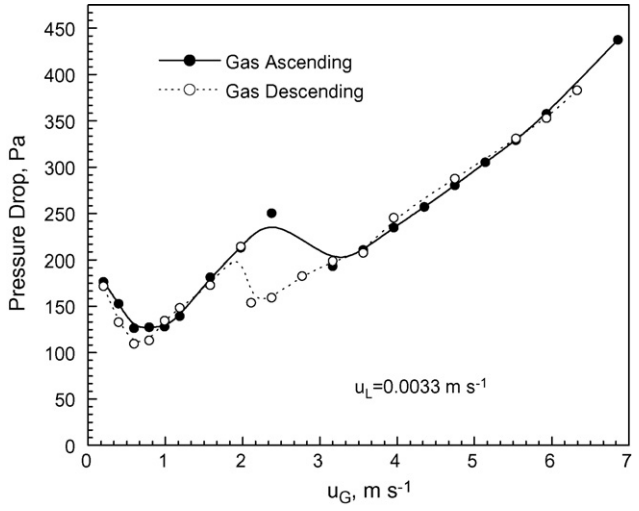

Fig. 3. Pressure drop versus gas velocities at $u_L = 0.0033\,m\,s^{-1}$ ($\beta = 0^\circ$).

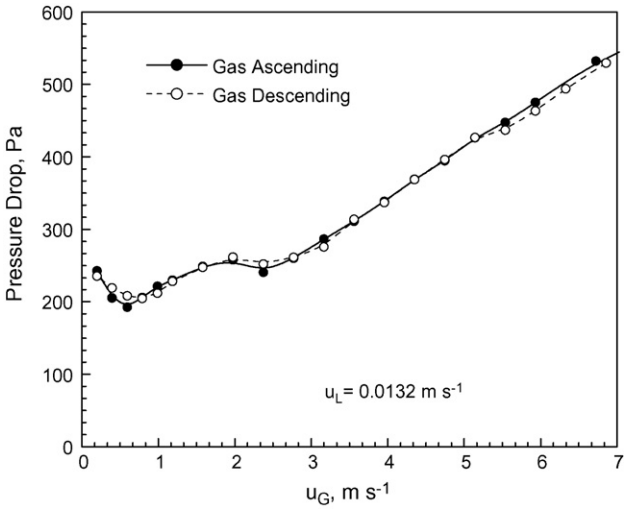

Fig. 4. Total pressure drop of two-channel system versus gas velocities at $u_L = 0.0132\,m\,s^{-1}$ ($\beta = 0^\circ$).

flow hysteresis region compared to that at $u_L = 0.0016\,m\,s^{-1}$. In addition, the pressure drop in Fig. 3 does not exhibit a monotonic increase with an increase in the superficial gas velocity at low gas velocities. A negative slope of the pressure drop is observed at relatively low gas velocities. The presence of the negative slope of the pressure drop versus superficial gas velocities is considered to be associated with flow mal-distribution and flow hysteresis. At relatively high liquid flow rates the flow hysteresis disappears as shown in Fig. 4 for $u_L = 0.0132\,m\,s^{-1}$. It clearly shows that the presence of liquid helps to mitigate the flow hysteresis in two-phase flow systems. The disappearance of a sudden change of the pressure drop versus gas flow rate also indicates an even distribution of gas and liquid flow in the two channels, as confirmed from measured liquid flow in the two channels, respectively, from the collection and weight method. In all cases for different liquid flow rates, the transition to uniform flow distribution for the ascending gas flow rate occurs at a pressure drop of 240 Pa. This appears to reflect an intrinsic characteristic of the current channel design which is believed to be a function of channel properties, such as surface roughness, wall wettability, channel orientation, etc.

3.1.2. Effects of inclination angles on pressure drop

It is shown in Fig. 5 that with an increase in inclined angles the total pressure drop increases due to the additional gravitational or static pressure drop. In addition, the hysteresis zone still exists in parallel channels inclined with a positive angle whereas flow hysteresis disappears at negative angles. The gravitational effect

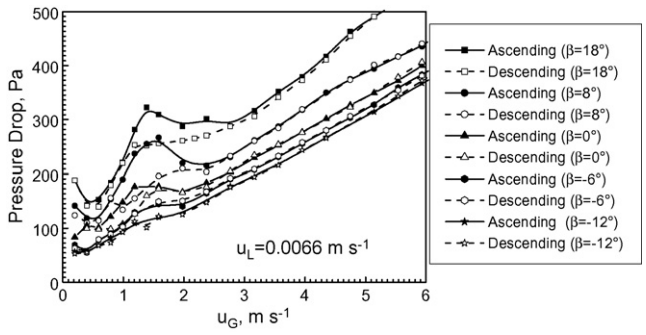

Fig. 5. Effects of inclination angles on the total pressure drop of the two-channel system.

on flow distribution is discussed in greater detail in the following section.

3.2. Liquid flow rate distribution

3.2.1. Effects of liquid flow rates on flow distribution

Distribution of liquid flow rate into the two channels was measured at different gas and liquid flow rates by the collection and weight method as described in the experimental section. The two channels were designated as channel 1 and channel 2, respectively. A typical liquid flow distribution is shown in Fig. 6. Here, Q_L represents the liquid flow rate measured in one channel, $m^3\,s^{-1}$, while Q_{L0} is the total liquid flow rate introduced to the Y-branched system, $m^3\,s^{-1}$. Similar to the pressure drop measurement, the gas flow rate was varied following an ascending and a descending path, respectively. It is seen from Fig. 6 that there exists a region with a mal-distribution of liquid flow into the two parallel channels, and the distribution appear to be random. The random distribution of two channels in this figure indicates that the difference in the geometry of the two channels plays only a marginal role on inducing the flow mal-distribution in the present study. However, in practical applications, channel geometry heterogeneity may exist and contribute to the flow difference among parallel channels. As shown in Fig. 6, the even distribution of liquid flow occurs at a superficial gas velocity of higher than $2.8\,m\,s^{-1}$ in the gas flow ascending process, while in the flow descending process the even distribution of liquid flow occurs at gas velocities higher than $2.3\,m\,s^{-1}$. Similar to the results from pressure drop measurement, discrepancy in liquid flow distribution in the two different gas channels also provides further evidence on the existence of flow hysteresis in the present study. With respect to the liquid flow distribution in parallel channels, Ozawa et al. [11] maintained the same liquid flow rate in two parallel channels by injecting the same amount of liquid into two parallel channels independently in their experiments. Minzer et al. [9], on the other hand, assumed that the same splitting ratio of gas flow rate to liquid flow rate is maintained in each channel after splitting from a common inlet manifold in order to avoid trivial solutions in their numerical simulations. This assumption is automatically valid only at the even distribution of both gas and liquid flow but is not applicable when flow mal-distribution occurs.

At high liquid flow rates, even distribution occurs at lower gas flow rates. For example, at a liquid velocity of $0.0066\,m\,s^{-1}$ as shown in Fig. 7, even distribution occurs at a superficial velocity of higher than about $2.0\,m\,s^{-1}$ and the resulted hysteresis zone becomes smaller than in Fig. 6. As the liquid velocity further increases to $0.033\,m\,s^{-1}$, as shown in Fig. 8, there is no more a noticeable hysteresis in flow distribution. The absence of flow hysteresis at liquid velocities higher than $0.1\,m\,s^{-1}$ was also observed in the previous work from Pustylnik et al. [10].

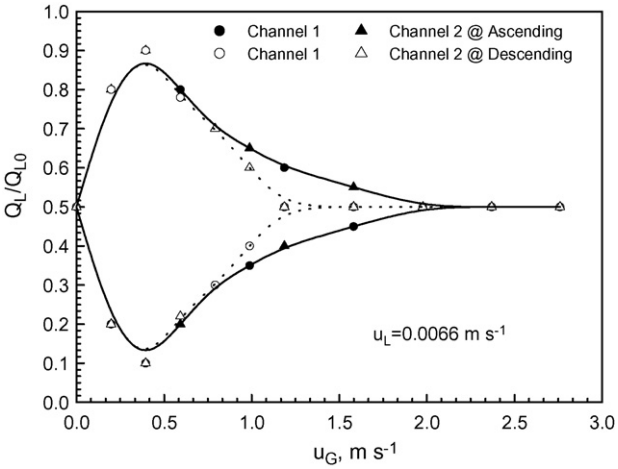

Fig. 7. Liquid flow distribution in two parallel channels ($\beta = 0^\circ$ and $u_L = 0.0066\,m\,s^{-1}$); solid line for flow ascending and dotted line for flow descending.

3.2.2. Effects of inclination angles on liquid flow distribution

A set of representative curves are shown in Fig. 9 to illustrate the gravity effect on flow distribution in the two parallel channels. It is seen clearly that with an increase in the inclination angle, the hysteresis zone increases and an even distribution is only achieved at higher gas velocities. For a negative slope of the channels, the flow hysteretic zone shrinks, and largely disappears when the inclined angle is changed to a negative value of 12°, indicating that the liquid flow is evenly distributed in the two parallel channels. The implication of these observations for fuel cell operations is that a slightly downward inclined flow field should help in water removal and uniform flow distribution.

The minimum gas flow rate required for even liquid flow distribution in the two parallel channels at various liquid velocities is generalized in Fig. 10. An even distribution region is located above the lines while a non-even distribution region is located underneath the lines.

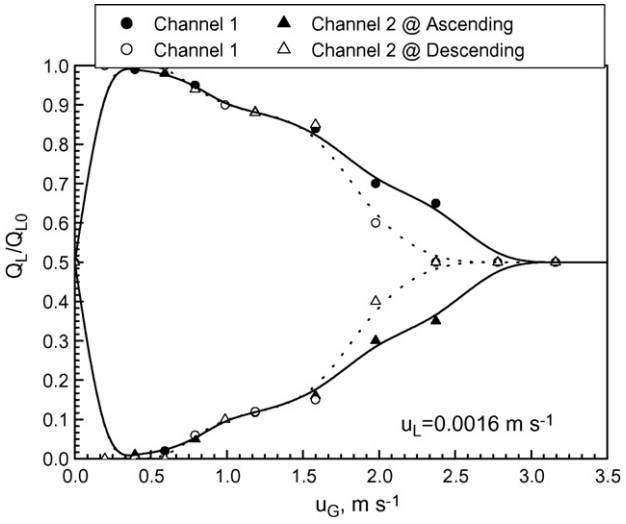

Fig. 6. Liquid flow distribution in two parallel channels ($\beta = 0^\circ$ and $u_L = 0.0016\,m\,s^{-1}$); solid line for flow ascending and dotted line for flow descending.

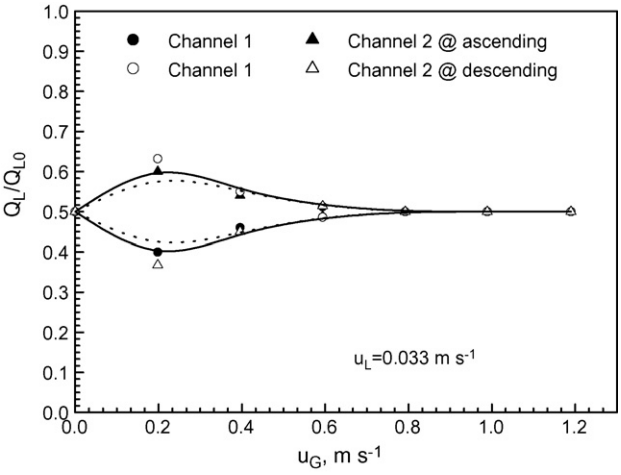

Fig. 8. Liquid flow distribution in two parallel channels ($\beta = 0^\circ$ and $u_L = 0.033\,m\,s^{-1}$); solid line for flow ascending and dotted line for flow descending.

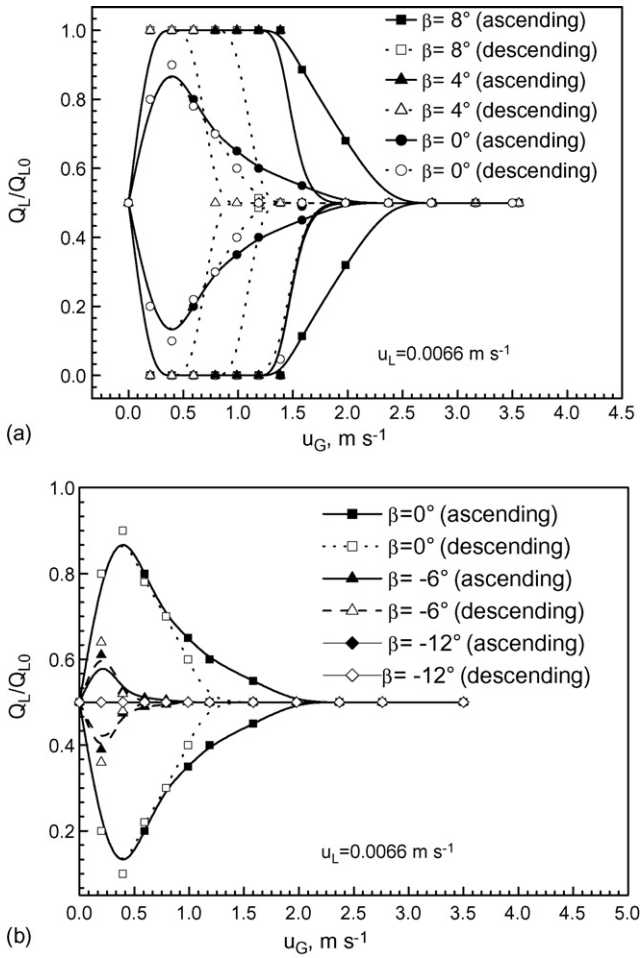

Fig. 9. Liquid distribution in two-parallel channels at $u_L = 0.0066\ m\ s^{-1}$: (a) $\beta = 0°$, 4° and 8°; (b) $\beta = 0°$, −6° and −12°.

It is shown in Fig. 10 that the inclination angle plays a complex role on flow distribution in parallel flow channels. The dimensionless Bond number provides information on influences of gravity on flow patterns/regimes and is given by

$$B_o = \frac{\rho g D_h^2}{\sigma} \quad (3)$$

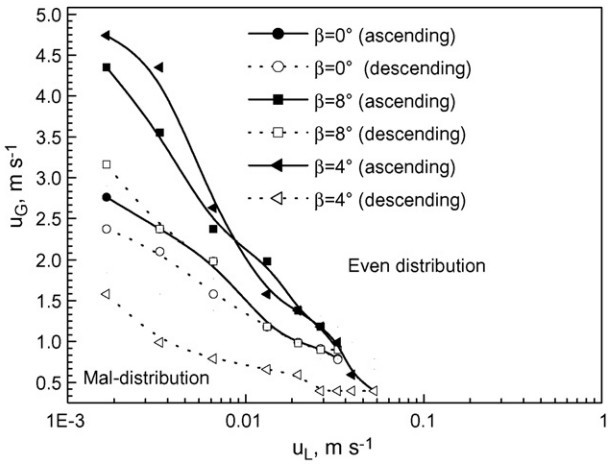

Fig. 10. Minimum gas velocities required for even liquid flow distribution between two channels.

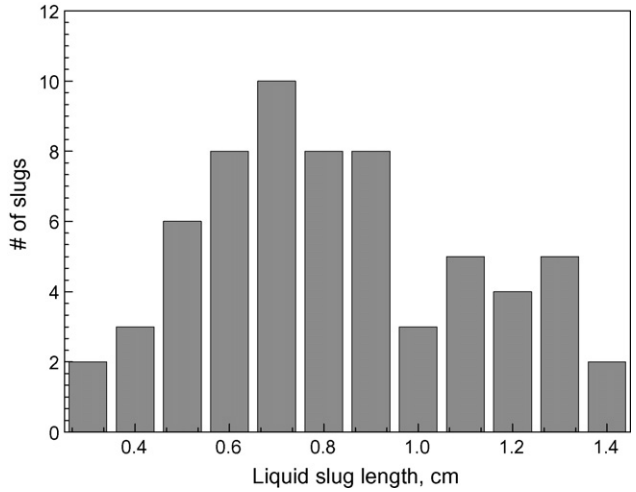

Fig. 11. Liquid slug length distribution at $u_L = 0.0066\ m\ s^{-1}$ and $u_G = 0.197\ m\ s^{-1}$.

where ρ is the liquid density (kg m^{-3}), and D_h is the hydraulic diameter (m), g is the gravitational rate. In the current experimental setup, the Bond number is 0.34, indicating that gravity might exert an impact on the flow patterns/regimes in the flow channel [13]. It is well known that pressure drop and gas holdup generally depend on flow regimes and gravity also imposes an additional influence due to the static pressure drop across the flow channel.

It is seen from this work that a higher gas flow rate is required to ensure an even liquid flow distribution in two parallel channels for a lower liquid flow rate. Therefore, in order to ensure the even distribution of gas and liquid flow, a high gas flow rate is required for the low liquid flow rate, typically encountered in fuel cells.

3.3. Liquid slugs and gas holdup

In the current experiments with the superficial liquid velocity ranging from 0.001 to 0.03 m s^{-1} and superficial gas velocities from 0.1 to 10 m s^{-1}, the following flow patterns were observed: slug flow, slug-to-annular flow, and annular flow, which are consistent with the previous studies of Triplett et al. [13] in semi-triangular channels with D_h = 1.49 mm and Barajas and Panton [14] in 1.6 mm diameter circular channels. This was discussed in our previous work [12]. In the slug flow regime, liquid slugs were analyzed in terms of liquid slug length and frequency. Typical distributions of the liquid slug length are shown in Figs. 11 and 12.

It can be seen that a narrower distribution of slug length exists at high liquid flow rate and the slug frequency is also higher at a higher liquid flow rate. A liquid slug frequency of 0.52 Hz is obtained for $u_L = 0.0066\ m\ s^{-1}$ and $u_G = 0.197\ m\ s^{-1}$ with an averaged slug length of 8.2 mm, while a slug frequency of 1.53 Hz is obtained at $u_L = 0.0196\ m\ s^{-1}$ and $u_G = 0.098\ m\ s^{-1}$ with an averaged slug length of 8.3 mm. Based on the slug velocity, slug length and slug frequency, liquid and gas fractions are estimated by Eq. (2), giving liquid fractions of 0.057 and 0.31 for the above two conditions, respectively.

In the literature, a large number of correlations or models have been reported for the prediction of gas holdup (volumetric gas fraction) in minichannels and microchannels [15–17]. However, caution should be exercised when those correlations are employed since they largely depend on flow regimes, channel geometries, and the physical properties of the gas and liquid phases. Among those correlations, the homogenous model based on no-slip condition between the gas and liquid phase is typically used as a base line as expressed

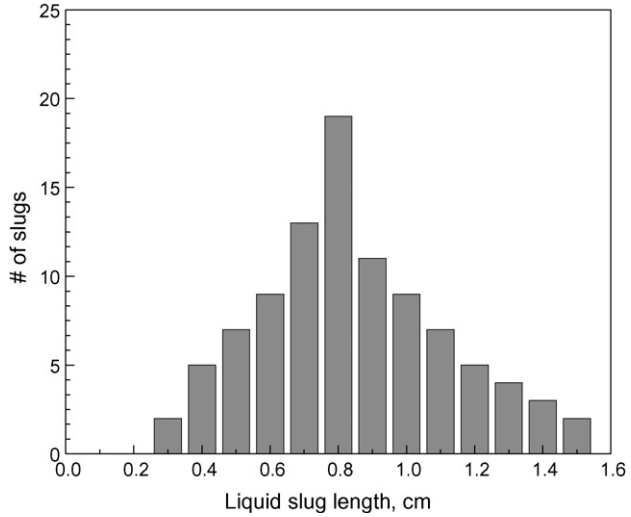

Fig. 12. Liquid slug length distribution at $u_L = 0.0196\ m\ s^{-1}$ and $u_G = 0.098\ m\ s^{-1}$.

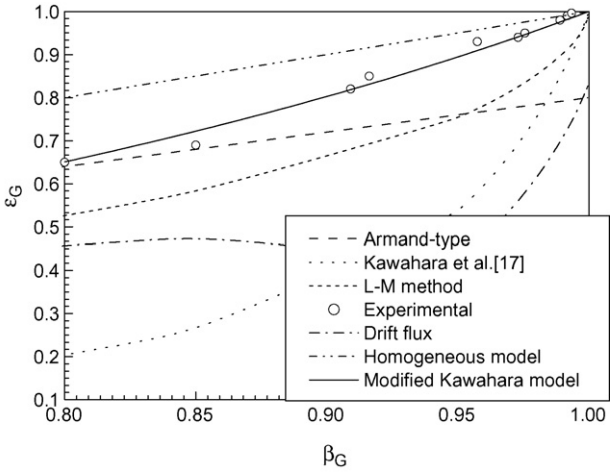

Fig. 13. Comparison of gas holdup predictions with experimental data.

in the following equation for the gas holdup β_G:

$$\beta_G = \frac{Q_G}{Q_L + Q_G} \tag{4}$$

where Q_L, Q_G denote the volumetric flow of the liquid and gas phase ($m^3\ s^{-1}$), respectively. The gas holdup can also be estimated by an Armand-type correlation in channels of diameter D_h greater than 1 mm [18] as follows:

$$\varepsilon_G = 0.83\beta_G \tag{5}$$

The drift flux model is indicated in the following equation:

$$\varepsilon_G = \frac{U_{GS}}{C(U_{GS+} + U_{LS}) + U_d} \tag{6}$$

where C is the distribution factor and equal to 1.2 for slug flow conditions, U_d is the drift flux velocity ($m\ s^{-1}$), which is the velocity of an elongated bubble in stagnant liquid, and is estimated by the following equation:

$$U_d = 0.54\cos\ \beta\sqrt{gD_h} + 0.35\sin\ \beta\sqrt{gD_h} \tag{7}$$

In general, the drift flux velocity in minichannels with diameter less than 5 mm can be neglected and Eq. (6) becomes the same as the Armand-type correlation as shown in Eq. (5).

The original Lockhart–Martinelli [19] relationship for gas fraction in an air-water system is given by

$$\varepsilon_G = \frac{0.45(Q_G/Q_L)^{0.65}}{1 + 0.45(Q_G/Q_L)^{0.65}} \tag{8}$$

Based on experimental data in microchannels with diameters of around 0.1 mm, Kawahara et al. [17] developed a non-linear relationship between gas fraction and homogenous gas holdup as follows:

$$\varepsilon_G = \frac{0.03{\beta_G}^{0.5}}{1 - 0.97{\beta_G}^{0.5}} \tag{9}$$

The above-mentioned correlations were used to compare with our current experimental data as shown in Fig. 13.

It is seen in the figure that all models/correlations underestimate gas holdup data and overestimate liquid holdup data compared to our experiment data. However, the homogenous model overestimates gas holdup data at lower values but agrees well with our experimental data at very dilute conditions at high gas to liquid flow ratios. An attempt was also made to correlate our experimental data using the Kawahara et al non-linear type expression, and a modified correlation was obtained with an averaged relative residue of less than 5 % as follows:

$$\varepsilon_G = \frac{0.22{\beta_G}^{0.5}}{1 - 0.78{\beta_G}^{0.5}} \tag{10}$$

Eq. (10) will be applied to predict the flow properties of gas–liquid mixture in the following section.

4. Theoretical considerations for flow distributions

Experimental results have shown that flow mal-distribution exists at low liquid and gas flow rates. In principle, even flow distribution in each channel satisfies the requirement for equal pressure drops across parallel channels sharing the same inlet and outlet. However, even distribution is not always observed in practice, and instead more gas or liquid flows into some channels than others. The flow pattern observed in practice should be stable since unstable solutions are unlikely present due to the fact that perturbations always exist in the system which can shift an unstable state to a new stable one. Therefore, flow distribution among parallel channels should be determined by flow stability rather than the criterion of a minimal pressure drop. Similar phenomena can occur in other multiphase flow systems such as gas-solid systems. Grace et al. [20] reported similar phenomena of gas and solid mal-distribution in parallel cyclones. The minimum pressure drop is sometime not the determinant of uniform flow distribution. Even a significant difference in flow distribution could lead to a very narrow range of pressure drop especially in dilute disperse phase systems.

In order to investigate flow distribution of two-phase flow in parallel channels, approximate momentum equations similar to the approaches used by several previous researchers [10,11] are used with the momentum balance across a single channel related to the total force exerting on the system by:

$$A(P_i - P_e) = M\frac{dU}{dt} + \tau SL + KA\rho\frac{U^2}{2} + \rho gLA\sin\ \beta \tag{11}$$

where P_i and P_e are the inlet and outlet pressure (Pa), respectively. M is the mass of the mixture in each channel (=ρAL) (kg), U is the average velocity of gas and liquid mixture ($m\ s^{-1}$), A is the cross-sectional area (m^2), L is the length of each channel (m), and S is the perimeter of the channel (m), τ is the wall shear stress (β) is the inclination angle (°), and K is a lumped dimensionless parameter due to flow turns within the channel and its magnitude is a function of turning angles or a number of bends in the system. In addition, for the purpose of simplicity, the pressure drop due to acceleration

is not considered since its contribution to the overall pressure drop is not significant. The shear stress can be evaluated by the following equation:

$$\tau = f\frac{\rho U^2}{2} \tag{12}$$

where f is the frictional factor which is a function of flow conditions, and

$$U = \frac{Q}{A} \tag{13}$$

where Q is the total volumetric gas and liquid flow rates in one channel ($m^3\ s^{-1}$). The averaged density of the mixture is evaluated by the following equation:

$$\rho = (1-\varepsilon_G)\rho_L + \varepsilon_G\rho_G \tag{14}$$

and similarly, the averaged viscosity is given by:

$$\mu = (1-\varepsilon_G)\mu_L + \varepsilon_G\mu_G \tag{15}$$

where ε_G is evaluated by the developed correlation as indicated in Eq. (10).

For a two parallel identical channel system, the momentum equation for channel 1 is

$$A(P_i - P_e) = M_1\frac{dU_1}{dt} + f_1\frac{\rho_1 {U_1}^2}{2}SL + KA\frac{\rho_1 {U_1}^2}{2} + \rho_1 gLA\sin\ \beta \tag{16}$$

Similarly, for channel 2,

$$A(P_i - P_e) = M_2\frac{dU_2}{dt} + f_2\frac{\rho_2 {U_2}^2}{2}SL + KA\frac{\rho_2 {U_2}^2}{2} + \rho_2 gLA\sin\ \beta \tag{17}$$

where A is the cross-sectional area of each channel (m^2) and M_1, M_2 are the total mass in the two channels, respectively. K is used to characterize the pressure drop due to geometry change along channels such as bends and turns and it is also a function of flow conditions [1]. It can be expected that in a typical serpentine PEM fuel cell flow field, K value should be related to the number of bends involved. In the current setup, K was experimentally estimated to be 1.0 from the pressure drop data of a single-phase gas system.

At steady state, the equal pressure drop for both channels leads to

$$f_1\frac{\rho_1 {U_1}^2}{2A}SL + K\frac{\rho_1 {U_1}^2}{2} + \rho_1 gL\sin\ \beta = f_2\frac{\rho_2 {U_2}^2}{2A}SL + K\frac{\rho_2 {U_2}^2}{2} + \rho_2 gL\sin\ \beta \tag{18}$$

It implies that any distribution of gas and liquid flow in the two parallel channels must satisfy Eq. (18). By defining Q_1 and Q_2 as the total volumetric flow rates of gas–liquid mixture in channel 1 and channel 2, $m^3\ s^{-1}$, respectively, we have,

$$Q_1 = Q_{L1} + Q_{G1} \tag{19}$$

$$Q_2 = Q_{L2} + Q_{G2} \tag{20}$$

Mass conservation for gas and liquid phases gives

$$Q_{L0} = Q_{L1} + Q_{L2} \tag{21}$$

$$Q_{G0} = Q_{G1} + Q_{G2} \tag{22}$$

where Q_{L0} and Q_{G0} are denoted as the total liquid and gas flow rates ($m^3\ s^{-1}$).

Similar to single-phase flow, f_1 and f_2 are the frictional factors related to Reynolds numbers in the two channels; in the laminar flow regime, fRe is equal to 14.2 for channels of square cross-section instead of circular calculated from [21]:

$$f\mathrm{Re} = 24(1 - 1.3553\alpha + 1.9467\alpha^2 - 1.7012\alpha^3 + 0.9564\alpha^4 - 0.2537\alpha^5) \tag{23}$$

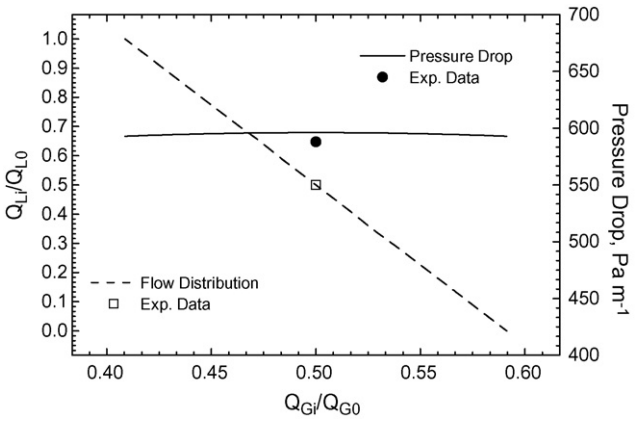

Fig. 14. Predicted and measured flow distribution in two horizontal parallel channels at $u_L = 0.0066\ m\ s^{-1}$ and $u_G = 4.74\ m\ s^{-1}$ (dot line: calculation for the flow distribution in one channel; solid line: calculation for the pressure drop across two-channel system).

where α is the geometry factor, and equal to 1 for a square cross-section.

For given liquid flow rates or gas flow rates in one channel, flows in the other channel can be obtained by solving Eq. (18) in combination with the mass balance Eqs. (21) and (22). At the same time, the pressure drop across the parallel channels is also obtained at corresponding flow distributions. Representative distribution curves calculated from the above approach are shown in Figs. 14 and 15. Q_{Li} and Q_{Gi} represent liquid flow rate and gas flow rate in channel i of the two channels. Experimental data has also been plotted in the figures for purposes of comparison.

It can be seen in Fig. 14 that for horizontal channels different combinations of gas and liquid flow rates in individual channels result in a very small variation in the total pressure drop across the channels at the given flow condition over a broad range of liquid flow fractions ranging from 0 to 1. In contrast, the variation of gas flow fraction is confined to a relatively narrow range of 0.4 to 0.6. Experimentally, the even flow distribution in the two channels was observed in both the gas flow ascending and descending processes. In Fig. 15, flow hysteresis phenomena were observed both theoretically and experimentally. The pressure drop can be significantly different depending on the flow distribution. As shown in this figure, the unit pressure drop can be 175 Pa m^{-1} for an evenly distributed flow or around 330 Pa m^{-1} for the extreme case when the majority of gas and liquid flow preferably to one channel, leading

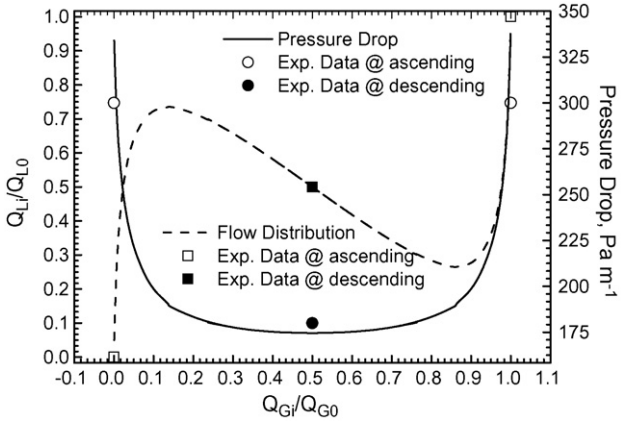

Fig. 15. Predicted and measured flow distribution in two parallel channels with an inclination angle of $\beta = 4°$ at $u_L = 0.0066\ m\ s^{-1}$ and $u_G = 0.79\ m\ s^{-1}$(dot line: calculation for the flow distribution in one channel; solid line: calculation for the pressure drop across two-channel system).

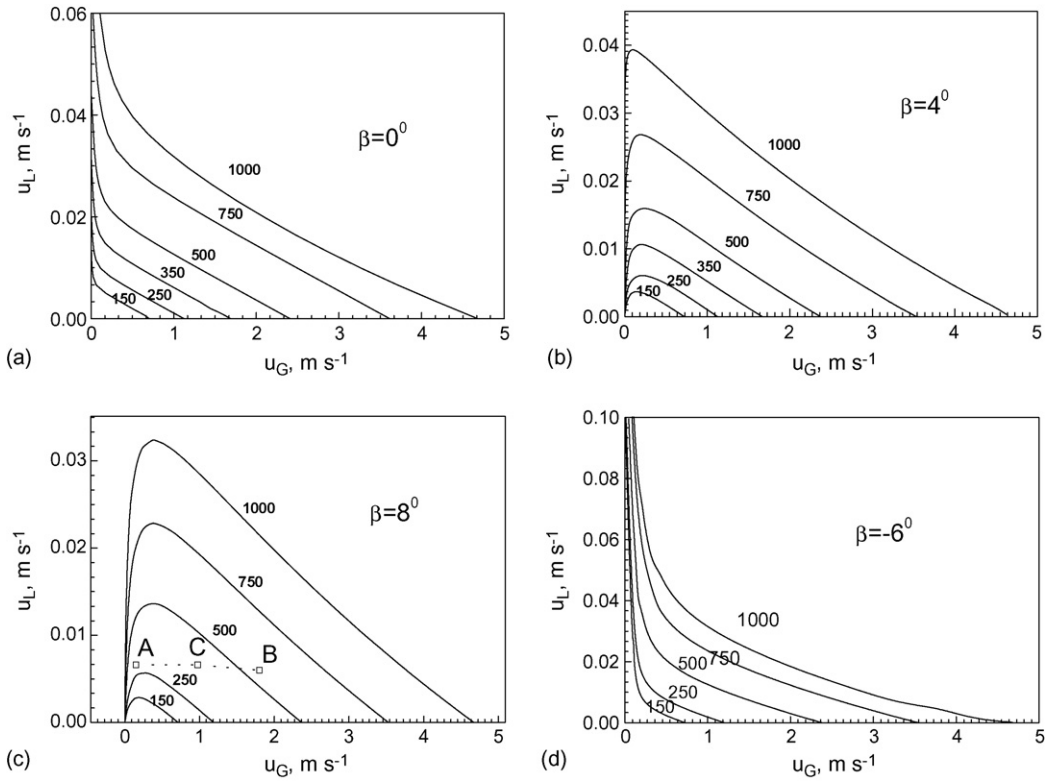

Fig. 16. Different isobaric contour (150–1000 Pa m^{-1}) with $K = 1$: (a) horizontal parallel channels; (b) parallel channels with an inclination angle of 4°; (c) parallel channels with an inclination angle of 8°; (d) parallel channels with an inclination angle of negative 6°.

to flooding in the other channel as demonstrated experimentally [12]. This result seems to suggest that the flow distribution into the two channels does not necessarily seek a minimum pressure drop in the system. Instead, flow stability along with initial conditions are likely key factors determining the flow distribution in two-phase parallel flow channels, which could be a unique characteristic of non-linear two-phase flow systems. In more general terms, if a small perturbation can shift one condition to another, it means that this condition is not stable. Otherwise, the condition is stable, as discussed by Pustylnik et al. [11]. More specifically, at regions where the slope of the pressure drop versus the flow rate curve is negative, a small disturbance in the gas flow rate can lead to a decrease in the pressure drop and triggers more gas flow into that channel. Consequently, it deviates from its original flow distribution and moves to another condition. This can be seen more clearly from the plot of isobars constructed by all solutions satisfying Eq. (18), namely, the solutions for an equal pressure drop. In Fig. 16, isobars at different inclination angles are presented.

The results in this figure show that the inclination angle has a significant impact on the shape of isobars, especially, at positively inclination angles, i.e., Fig. 16(b) and (c). When the gas velocity increases at a constant liquid velocity, the pressure drop decreases initially, followed by an increase. It can be seen that point A in Fig. 16(c) is unlikely to be observed in experiments because it is located in the negative slope region while point B is a stable solution because of its location in isobars. In addition, point A and point B do not coexist since they are not a pair of solutions of Eq. (18). However, their median could be observed as point C in this figure since it is located in the stable region. Therefore, the approach developed here can be used not only for the evaluation of the stability of even flow distributions in parallel channels but also for the identification of the possibility of flow mal-distribution.

5. Applications to fuel cells

There are many types of flow field designs in PEMFCs, with straight channels and serpentine channels being the most common ones. The application of the procedure developed above to typical fuel cell flow fields was demonstrated through the following two cases, with one for two straight parallel channels and the other for two serpentine channels with the same length for both types of channels. For serpentine channels, an additional pressure drop is induced from channel bends compared to the straight channels. For the purpose of demonstration, all turns were simplified to 90° bends. For a flow field consisting of a square cross-section of 1.59 mm × 1.59 mm with a length of 45 cm, the equivalent active area is around 15 cm^2. The simulated results are shown in Fig. 17.

It can be seen in Fig. 17 that pressure drops in serpentine channels are generally higher than in straight channels, because of the additional pressure drop contributed from the channel bends compared to straight channels. However, it seems that the gas flow distribution is confined to a narrower range in straight channels compared to serpentine channels. For example, in Fig. 17(a), the range of gas flow distribution in straight channels is from 0.486 to 0.514 while it is from 0.480 to 0.520 for serpentine channels. The pressure drop in serpentine channels is around 400 Pa m^{-1} while it is about 350 Pa m^{-1} in straight channels in Fig. 17(a) and it is around 1780 Pa m^{-1} in serpentine channels whereas it is about 1035 Pa m^{-1} in straight channels as shown in Fig. 17(b). At a higher gas to liquid flow ratio (equivalent to higher gas stoichiometry), gas flow is distributed in a narrower range of from 0.505 to 0.495 in Fig. 17(b), compared to the range from 0.520 to 0.480 at a lower gas-to-liquid flow ratio or lower stoichiometry shown in Fig. 17(a) for straight channels. Although in PEMFCs, a higher pressure drop in serpentine channels sometimes is beneficial for liquid water removal, it can be seen that in order to ensure even flow distribution, higher gas to liquid flow ratio is required regard-

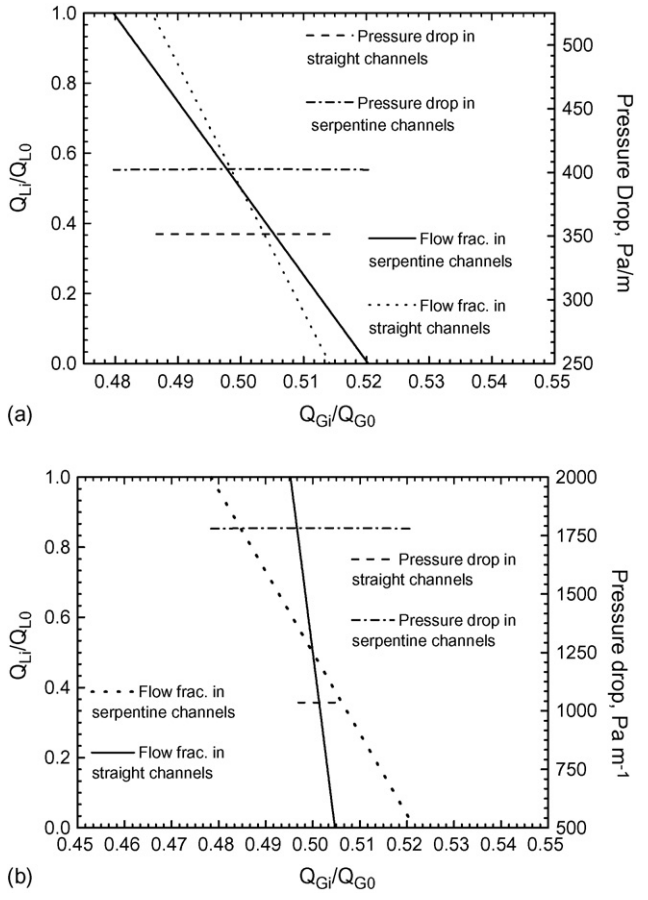

Fig. 17. Comparison of flow distributions in straight channels and serpentine channels of the same length (a) $Q_{L0} = 0.125\,\mathrm{ml\,min^{-1}}$ and $Q_{G0} = 500\,\mathrm{ml\,min^{-1}}$ (corresponding current density of $0.78\,\mathrm{A\,cm^{-1}}$ and gas stoichiometry of 2.75); (b) $Q_{L0} = 0.125\,\mathrm{ml\,min^{-1}}$ and $Q_{G0} = 1500\,\mathrm{ml\,min^{-1}}$ (corresponding current density $0.78\,\mathrm{A\,cm^{-1}}$ and gas stoichiometry of 7.75).

less of flow field configurations: serpentine channels or straight channels.

6. Conclusions

Gas liquid two-phase flow distribution in parallel channels related to fuel cell applications was studied. It was found that flow mal-distribution and flow hysteresis occur at low gas and liquid flow velocities. When varying channel orientation, gravitational force shows a significant impact on the flow distribution as well as on the flow hysteresis. In general, a higher gas flow rate is required to ensure even flow distribution to the two parallel channels with a positively inclined angle while a negatively inclined angle helps in reducing the flow mal-distribution. A two-phase flow hydrodynamic model is used to evaluate flow distribution based on the equal pressure drop criterion. It was found that unstable flow distributions are located at regions where there is a negative slope of pressure drop versus the flow rate curve, leading to uneven flow distribution or flooding in one channel. The actual flow distribution to two parallel channels highly depends on flow stability and initial conditions. The developed approach was used to compare two typical fuel cell flow fields: straight channels and serpentine channels. In terms of flow distribution, straight channels perform slightly better than serpentine channels. However, higher pressure drop in serpentine channels is sometime beneficial for liquid water removal. For both types of flow fields, however, a higher gas flow rate or gas stoichiometry is required in order to achieve even distribution across flow channels. Further studies on the effect of channel properties such as wettability and geometry on flow mal-distribution are still required for optimal flow field design.

Acknowledgements

The authors are grateful to a strategic grant from the Natural Sciences and Engineering Research Council of Canada (NSERC) to support this work.

References

[1] S. Maharudrayya, S. Jayanti, A.P. Deshpande, J. Power Sources 138 (2004) 1–13.
[2] S. Maharudrayya, S. Jayanti, A.P. Deshpande, J. Power Sources 144 (2005) 94–106.
[3] S. Maharudrayya, S. Jayanti, A.P. Deshpande, J. Power Sources 157 (2006) 358–367.
[4] S. Ge, C.Y. Wang, J. Electrochem. Soc. 154 (2007) B998–B1005.
[5] Y. Wang, S. Basu, C.Y. Wang, J. Power Sources 179 (2008) 603–617.
[6] M. Tshuva, D. Barnea, Y. Taitel, Int. J. Multiphase Flow 25 (1999) 1491–1503.
[7] Y. Taitel, L. Pustylnik, M. Tshuva, D. Barnea, Int. J. Multiphase Flow 29 (2003) 1193–1202.
[8] U. Minzer, D. Barnea, Y. Taitel, Int. J. Multiphase flow 30 (2004) 763–777.
[9] U. Minzer, D. Barnea, Y. Taitel, Chem. Eng. Sci. 61 (2006) 7259–7429.
[10] L. Pustylink, D. Barnea, Y. Taitel, AIChE J. 52 (2006) 345–3352.
[11] M. Ozawa, K. Akagawa, T. Sakaguchi, Int. J. Multiphase Flow 15 (1989) 639–657.
[12] L.F. Zhang, H.T. Bi, D.P. Wilkinson, J. Stumper, H.J. Wang, J. Power sources 183 (2008) 643–650.
[13] A. Triplett, S.M. Ghiaasiaan, S.I. Adbel-Khalik, D.L. Sadowski, Int. J. Multiphase Flow 25 (1999) 377–394.
[14] A.M. Barajas, R.L. Panton, Int. J. Multiphase Flow 19 (1993) 337–346.
[15] J.J.J. Chen, P.L. Spedding, Int. J. Multiphase Flow 9 (1983) 147–159.
[16] K.A. Treplett, S.M. Ghiaasiaan, S.I. Abdel-Khalik, A. LeMouel, B.N. McCord, Int. J. Multiphase Flow 25 (1999) 395–410.
[17] A. Kawahara, P.M.Y. Chung, M. Kawaji, Int. J. Multiphase Flow 28 (2002) 1411–1435.
[18] M.I. Ali, M. Sadatomi, M. Kawaji, Can. J. Chem. Eng. 71 (1993) 657–666.
[19] R.W. Lockhart, R.C. Martinelli, Chem. Eng. Prog. 45 (1949) 39–48.
[20] J. Grace, H. Cui, S.S.E.H. Elnashaie, Can. J. Chem. Eng. 85 (2007) 662.
[21] S. Kakac, R.K. Shah, W. Aung, Handbook of Single-phase Convective Heat Transfer, Wiley, New York, 1987.